Supporting Information: Electrochemical Performance and Structures of Cr and Mo Doped ε-Li_xVOPO_4 Predicted as Promising Cathodes for Next Generation Lithium-ion Batteries

Vedanth B. Iyer,† William A. Goddard III*

Materials and Process Simulation Center, MC 137-74,

California Institute of Technology, Pasadena, CA 91125, United States

†permanent address, Portland OR

*E-mail: wag@caltech.edu

Table of Contents

DFT Relaxed Structures and Atomic Coordinates

Table S1. DFT (PBE+U) calculated unit cell parameters for Li_xVOPO_4 in comparison with previous experimental [1] and QM (HSE) [1] lattice parameters

Lithium Content (x)	Data Type	a (Å)	b (Å)	c (Å)	α (°)	β (°)	γ (°)	Volume(Å³)
0	PBE+U	7.356	7.006	7.364	90.00	115.14	90.00	343.52
	Exp.	7.266	6.893	7.265	90.00	115.30	90.00	329.10
	HSE	7.246	6.966	7.308	90.00	114.62	90.00	335.36
1	PBE+U	6.845	7.218	8.010	89.73	91.60	116.51	353.94
	Exp.	6.734	7.196	7.918	89.81	91.27	116.91	342.04
	HSE	6.870	7.159	7.825	89.79	91.31	117.24	342.06
1.5	PBE+U	7.132	7.199	7.805	90.14	90.44	116.17	359.70
	Exp.	6.982	6.992	7.789	89.57	89.90	115.72	342.54
	HSE	6.968	7.014	7.770	89.65	89.08	116.22	340.58
2	PBE+U	7.191	7.327	7.864	90.11	90.48	116.18	371.84
	Exp.	7.195	7.101	7.775	89.82	89.79	116.34	356.00
	HSE	7.250	7.106	7.714	89.68	90.01	116.34	356.16
2.5	PBE+U	7.402	7.618	7.809	91.31	90.32	118.12	388.20
	Exp.	n/a	n/a	n/a	n/a	n/a	n/a	n/a
	HSE	n/a	n/a	n/a	n/a	n/a	n/a	n/a

Table S2. DFT (PBE+U) calculated unit cell parameters for stable phases of the doped Z-Li_xVOPO_4 structures

Lithium Content (x)	**System**	**a (Å)**	**b (Å)**	**c (Å)**	**α (º)**	**β (º)**	**γ (º)**	**Volume(Å³)**
0	Cr	7.356	7.030	7.373	90.05	115.00	89.97	345.58
	Mo	7.397	7.093	7.418	90.21	115.26	91.02	351.90
0.5	Mo_1	6.889	7.340	7.965	90.16	90.88	117.45	357.34
	Mo_2	6.886	7.327	7.970	90.74	90.31	117.28	357.33
1	Cr_1	6.809	7.098	8.031	89.85	91.27	116.02	348.72
	Cr_2	6.822	7.121	8.034	89.61	91.68	116.12	350.22
	Mo_1	6.861	7.164	8.080	89.65	91.65	115.86	357.21
	Mo_2	6.851	7.164	8.076	89.59	91.90	115.69	356.97
1.5	Cr_1	7.073	7.201	7.802	89.83	91.49	116.82	354.51
	Cr_2	7.082	7.188	7.812	90.17	90.76	116.70	355.19
	Mo_1	7.136	7.235	7.888	89.95	91.28	116.76	363.55
	Mo_2	7.145	7.232	7.884	90.49	91.07	116.77	363.58
2	Cr_1	7.184	7.316	7.830	89.90	90.83	116.32	368.81
	Cr_2	7.184	7.312	7.827	90.26	90.05	116.24	368.71
	Mo_1	7.249	7.381	7.888	89.94	90.84	116.42	377.87
	Mo_2	7.259	7.361	7.895	90.23	90.15	116.15	378.62
2.5	Cr_1	7.382	7.687	7.797	91.49	89.86	117.92	390.74
	Cr_2	7.329	7.660	7.780	90.48	89.68	116.12	392.16
	Mo_1	7.462	7.632	7.871	90.68	90.28	117.62	397.11
	Mo_2	7.488	7.643	7.871	91.36	90.21	118.33	396.28

Table S3. DFT (PBE+U) relaxed atomic positions of the distinct intermediate phases at Mo-$Li_{0.5}VOPO_4$. (a) structure with the Mo_1 dopant; (b) structure with the Mo_2 dopant.

Atom	x	y	z	Atom	x	y	z
Li	0.7859	0.7002	0.9191	Li	0.7843	0.6907	0.9194
Li	0.3218	0.8423	0.4274	Li	0.3038	0.8334	0.4278
V	0.2489	0.0359	0.7680	V	0.2482	0.0344	0.7682
V	0.7553	0.9706	0.2304	V	0.2380	0.5176	0.7387
V	0.2370	0.5178	0.7387	V	0.7566	0.4752	0.2664
P	0.2419	0.7541	0.0804	P	0.2313	0.7503	0.0809
P	0.7612	0.2423	0.9122	P	0.7608	0.2486	0.9104
P	0.2530	0.2368	0.4175	P	0.2664	0.2421	0.4178
P	0.7352	0.7634	0.5880	P	0.7370	0.7575	0.5871
O	0.5513	0.0894	0.8235	O	0.5517	0.0901	0.8253
O	0.4490	0.9100	0.1748	O	0.4396	0.9093	0.1759
O	0.1337	0.8551	0.9688	O	0.1281	0.8535	0.9685
O	0.8549	0.1337	0.0286	O	0.8596	0.1375	0.0216
O	0.9272	0.9059	0.7016	O	0.9282	0.9022	0.7003
O	0.0507	0.0900	0.3187	O	0.0633	0.0929	0.3160
O	0.3315	0.1084	0.5270	O	0.3359	0.1085	0.5273
O	0.6409	0.8667	0.4646	O	0.6408	0.8669	0.4699
O	0.2332	0.7278	0.6657	O	0.2346	0.7288	0.6673
O	0.7609	0.2554	0.3170	O	0.7625	0.2523	0.3187
O	0.2699	0.2612	0.8271	O	0.2687	0.2610	0.8267
O	0.7376	0.7405	0.1620	O	0.7359	0.7482	0.1630
O	0.0869	0.6431	0.2288	O	0.0782	0.6402	0.2279
O	0.9356	0.3645	0.7784	O	0.9347	0.3680	0.7757
O	0.2901	0.6040	0.9714	O	0.2872	0.6034	0.9711
O	0.7246	0.4083	0.1120	O	0.7269	0.4109	0.0157
O	0.4329	0.3702	0.2941	O	0.4440	0.3739	0.2957
O	0.5590	0.6286	0.7174	O	0.5598	0.6255	0.7172
O	0.2014	0.3863	0.5266	O	0.2051	0.3865	0.5263
O	0.8126	0.6289	0.4848	O	0.8123	0.6272	0.4781
Mo	**0.7560**	**0.4794**	**0.2658**	**Mo**	**0.7566**	**0.9842**	**0.2353**

(a) **(b)**

Table S4. DFT (PBE+U) relaxed atomic positions for all Z-$Li_{2.5}VOPO_4$ systems. (a) $Li_{2.5}VOPO_4$; (b) Cr_1-$Li_{2.5}VOPO_4$; (c) Cr_2-$Li_{2.5}VOPO_4$; (d) Mo_1-$Li_{2.5}VOPO_4$; (e) Mo_2-$Li_{2.5}VOPO_4$. Atomic coordinates of the additional Li atoms and dopants are highlighted in **bold face**.

Atom	x	y	z
Li	**0.3641**	**0.5155**	**0.1982**
Li	0.5000	0.5000	0.5000
Li	0.5000	0.0000	0.0000
Li	0.2501	0.1258	0.5385
Li	0.1426	0.6733	0.0568
Li	0.1394	0.4006	0.5563
V	0.0215	0.7777	0.7547
V	0.5011	0.7571	0.7536
P	0.7397	0.2278	0.6192
P	0.7528	0.7282	0.1176
O	0.1007	0.5639	0.3014
O	0.6571	0.0842	0.7686
O	0.4284	0.7430	0.4766
O	0.8590	0.1594	0.4953
O	0.7421	0.2179	0.1479
O	0.1048	0.0737	0.7867
O	0.4290	0.2678	0.9767
O	0.7444	0.7011	0.6400
O	0.6599	0.5724	0.2638
O	0.1308	0.3437	0.0085

(a)

Atom	x	y	z	Atom	x	y	z
Li	**0.3598**	**0.5101**	**0.1887**	**Li**	**0.3597**	**0.5119**	**0.2011**
Li	**0.6270**	**0.4878**	**0.8176**	**Li**	**0.6452**	**0.4856**	**0.7969**
Li	0.4994	0.4988	0.5013	Li	0.4954	0.4987	0.5004
Li	0.5003	0.0058	0.9991	Li	0.4987	0.9996	0.0017
Li	0.2515	0.1297	0.5409	Li	0.2448	0.1180	0.5433
Li	0.7495	0.8759	0.4612	Li	0.7459	0.8708	0.4533
Li	0.8593	0.3101	0.9397	Li	0.8640	0.3439	0.9477
Li	0.1432	0.6877	0.0607	Li	0.1480	0.6647	0.0537
Li	0.1387	0.4028	0.5537	Li	0.1317	0.3918	0.5606
Li	0.8655	0.4028	0.5537	Li	0.8625	0.5982	0.4480
V	0.0212	0.7709	0.7546	V	0.9795	0.2132	0.2421
V	0.9764	0.2190	0.2446	V	0.4995	0.7586	0.7533
V	0.4987	0.2436	0.2460	V	0.4997	0.2427	0.2479
P	0.7446	0.2380	0.6167	P	0.7315	0.2111	0.6171
P	0.2612	0.7750	0.3797	P	0.2578	0.7748	0.3816
P	0.2410	0.2605	0.8815	P	0.2551	0.2880	0.8809
P	0.7533	0.7258	0.1210	P	0.7552	0.7257	0.1168
O	0.1027	0.5677	0.3023	O	0.1094	0.5727	0.3028
O	0.9110	0.4502	0.6799	O	0.8810	0.4071	0.7004
O	0.6673	0.1087	0.7731	O	0.6469	0.0588	0.7598
O	0.3388	0.9173	0.2305	O	0.3491	0.9201	0.2340
O	0.4319	0.7483	0.4747	O	0.4237	0.7435	0.4840
O	0.5735	0.2607	0.5194	O	0.5650	0.2504	0.5242
O	0.8593	0.1597	0.4953	O	0.8545	0.1480	0.4879
O	0.1413	0.8423	0.5064	O	0.1290	0.8393	0.5021
O	0.7422	0.2160	0.1482	O	0.7470	0.2213	0.1482
O	0.2629	0.7843	0.8501	O	0.2743	0.7815	0.8518
O	0.0976	0.0584	0.7978	O	0.1191	0.1079	0.7780
O	0.8891	0.9235	0.2153	O	0.8907	0.9193	0.2099
O	0.4264	0.2653	0.9784	O	0.4334	0.2724	0.9754
O	0.5686	0.7225	0.0239	O	0.5788	0.7370	0.0170
O	0.7391	0.7035	0.6488	O	0.7311	0.7074	0.6451
O	0.2546	0.3001	0.3571	O	0.2534	0.2968	0.2624
O	0.6647	0.5699	0.2659	O	0.6571	0.5732	0.2657
O	0.3287	0.4061	0.7301	O	0.3529	0.4530	0.7407
O	0.1251	0.3349	0.0069	O	0.1374	0.3573	0.0128
O	0.8741	0.6599	0.9927	O	0.8763	0.6512	0.9957
Cr	**0.5048**	**0.7618**	**0.7538**	**Cr**	**0.0191**	**0.7814**	**0.7570**

(b) **(c)**

Atom	x	y	z	Atom	x	y	z
Li	**0.3618**	**0.5083**	**0.1956**	**Li**	**0.3612**	**0.5051**	**0.1826**
Li	**0.6387**	**0.4804**	**0.7852**	**Li**	**0.6233**	**0.4815**	**0.8001**
Li	0.4987	0.4972	0.4921	Li	0.4960	0.5048	0.4935
Li	0.4876	0.0025	0.0044	Li	0.4916	0.9991	0.0007
Li	0.2464	0.1179	0.5438	Li	0.2521	0.1272	0.5366
Li	0.7511	0.8757	0.4522	Li	0.7452	0.8764	0.4631
Li	0.8535	0.3376	0.9467	Li	0.8562	0.3059	0.9393
Li	0.1456	0.6680	0.0562	Li	0.1410	0.6765	0.0608
Li	0.1386	0.3922	0.5557	Li	0.1400	0.3954	0.5568
Li	0.8582	0.6044	0.4470	Li	0.8563	0.6020	0.4346
V	0.0178	0.7713	0.7544	V	0.9776	0.2219	0.2472
V	0.9793	0.2216	0.2440	V	0.5023	0.7603	0.7544
V	0.5010	0.2425	0.2485	V	0.5023	0.2432	0.2470
P	0.7417	0.2268	0.6160	P	0.7421	0.2306	0.6197
P	0.2567	0.7721	0.3810	P	0.2628	0.7726	0.3799
P	0.2472	0.2725	0.8843	P	0.2484	0.2769	0.8833
P	0.7562	0.7266	0.1176	P	0.7505	0.7245	0.1181
O	0.1069	0.5658	0.3002	O	0.1006	0.5649	0.3028
O	0.8940	0.4303	0.6980	O	0.9058	0.4382	0.6970
O	0.6564	0.0816	0.7643	O	0.6632	0.0908	0.7708
O	0.3499	0.9187	0.2372	O	0.3481	0.9172	0.2341
O	0.4212	0.7403	0.4821	O	0.4274	0.7439	0.4769
O	0.5745	0.2576	0.5223	O	0.5748	0.2580	0.5262
O	0.8606	0.1594	0.4937	O	0.8585	0.1605	0.4968
O	0.1347	0.8373	0.5005	O	0.1447	0.8443	0.5015
O	0.7463	0.2234	0.1508	O	0.7451	0.2194	0.1492
O	0.2768	0.7909	0.8675	O	0.2715	0.7916	0.8681
O	0.1126	0.0846	0.7842	O	0.1067	0.0784	0.7893
O	0.8905	0.9221	0.2135	O	0.8910	0.9226	0.2137
O	0.4272	0.2565	0.9800	O	0.4318	0.2790	0.9768
O	0.5800	0.7369	0.0198	O	0.5727	0.7264	0.0208
O	0.7302	0.6981	0.6294	O	0.7324	0.6985	0.6319
O	0.2545	0.2944	0.3611	O	0.2554	0.2955	0.3577
O	0.6548	0.5709	0.2622	O	0.6562	0.5681	0.2622
O	0.3440	0.4341	0.7400	O	0.3360	0.4312	0.7371
O	0.1309	0.3450	0.0091	O	0.1313	0.3440	0.0106
O	0.8728	0.6526	0.9975	O	0.8693	0.6533	0.9959
Mo	**0.5026**	**0.7585**	**0.7538**	**Mo**	**0.0183**	**0.7672**	**0.7532**

(d) **(e)**

Energetics and Electrochemical Performance

Based on previous studies and literature on computational battery theory [1,2] , we calculated the formation energies and constructed the convex hulls for all systems relative to the ε-Li_xVOPO_4 end members (x = 0 – 2). Equation 1 is used to derive the formation energy Δ*E (x)* at each phase:

$$\Delta E(x) = E(Li_xVOPO_4) - \frac{2-x}{2} * E(VOPO_4) - \frac{x}{2} * E(Li_2VOPO_4)$$

(1)

where E is defined as the total DFT energy of the system. We also calculated the formation energies in this manner for the dopant systems as well.

Furthermore, the DFT energetics can be used to obtain a theoretical voltage profile with increasing lithiation [2,3]. Equation 2 is used to derive the voltage step using two Li_xVOPO_4 reference points:

$$V = -\frac{E(Li_{x2}VOPO_4) - E(Li_{x1}VOPO_4) - (x2 - x1) * E(Li)}{(x2 - x1)e}$$

(2)

where E is again defined as the total DFT energy of the system and "e" is termed as the exact coulombic charge of an electron. Equation 2 thus provides an average change in voltaic behavior across the lithiation cycle.

The root-mean-squared deviation (RMSD) values for both delithation and relithiation were calculated using the initial structures with either the Li removed or added (reference system) and the reoptimized structures. Equation 3 is used to calculate the RMSD: [7]

$$RMSD = \sqrt{\frac{1}{N}\sum_{i=0}^{N}((v_{ix} - w_{ix})^2 + (v_{iy} - w_{iy})^2 + (v_{iz} - w_{iz})^2)}$$

(3)

where v and w are the vector coordinates in Å for the reference and reoptimized systems respectively and N is the total number of ions in the system.

DFT Constructed Convex Hull and Voltage Profiles for undoped Li_xVOPO_4

The DFT calculated formation energies and voltage profiles for Li_xVOPO_4 are generally consistent with previous experimental and theoretical works [1]. Figure S1 displays the constructed convex hull highlighting the formation energies of undoped Li_xVOPO_4 for stable phases of $VOPO_4$ to Li_2VOPO_4.

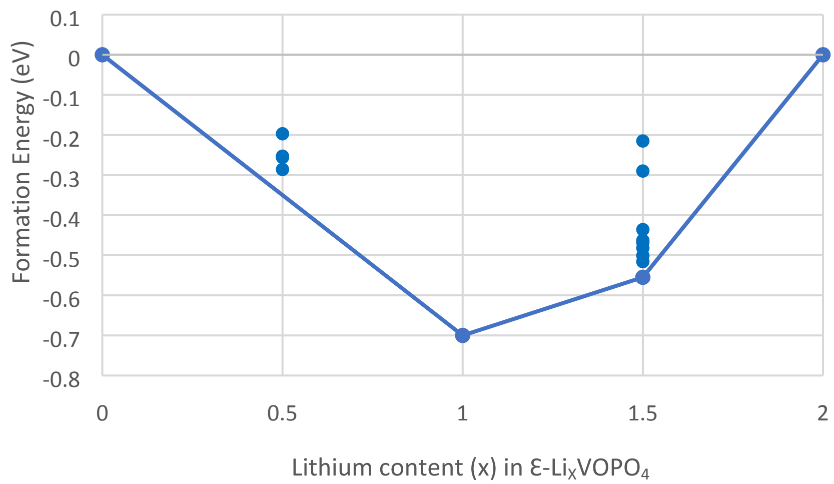

Figure S1. DFT (PBE+U) constructed convex hull showing the formation energies for the most stable configurations of ε-Li_xVOPO_4

We observe that going from the fully delithiated phase to the first lithium insertion, there are no stable intermediate configurations of Li_xVOPO_4 since the $Li_{0.5}VOPO_4$ phase displays a calculated formation energy above the convex hull. This is in agreement with previous experiments and QM studies [1,5]. We also note that the most stable phase of Li_xVOPO_4 is for the first lithium insertion (where x = 1). We further observe a stable intermediate phase at $Li_{1.5}VOPO_4$ between the first and second lithium insertion, which is also in agreement with previous experiments and QM studies [1].

The DFT calculated voltage profile for Li_xVOPO_4 shown in Table S5 is also in great agreement with previous experimental studies and QM calculations [1,6]. Table S5 compares our DFT (PBE+U) calculated voltage profiles with previous experimental values and hybrid DFT (HSE) calculations taken as an average over the entire lithiation cycle.

Table S5. Comparison of our calculated voltage profile (PBE+U) for ε-Li_xVOPO_4 as a function of the lithiation cycle

Charging Potential of ε-Li_xVOPO_4 as a function of (x)	DFT (PBE+U) Calculated (0K) (this work)	Experimental (298 K) [ref 1.]	DFT (HSE) Calculated (0K) [ref 1.]
0 - 0.5	3.73 V	3.8 - 4.5 V	4.01 V
0.5 - 1	3.73 V	3.8 - 4.5 V	4.01 V
1 - 1.5	2.74 V	2.37- 2.5 V	2.67 V
1.5 - 2	1.92 V	2.04 – 2.14 V	2.00 V
2 – 2.5	0.97 V	N/A	N/A

Here, we predict that the voltage step beyond the second lithium insertion (from 2 to 2.5) is around 1 V, suggesting that a higher lithium capacity is technically possible. This might not be realistic however because the electrolyte in such a battery would require a somewhat large electrochemical window that is lower than 1V and higher than 4V.

Local ZO_6 Octahedral Evaluation

Figures S2(a) – 2(c) highlight the local ZO_6 environments (where Z = V, Cr, or Mo) of the systems at the fully delithiated state and each Li insertion.

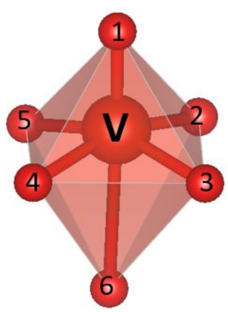

[1]

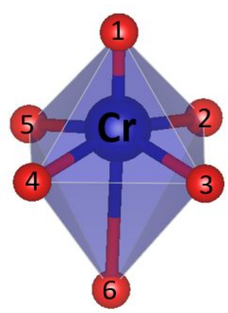

[2]

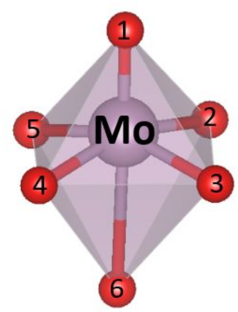

[3]

SYSTEM	Z-O_1 (Å)	Z-O_2 (Å)	Z-O_3 (Å)	Z-O_4 (Å)	Z-O_5 (Å)	Z-O_6 (Å)
VO_6 (V^{5+}) [1]	1.600	1.881	1.904	1.917	1.922	2.598
CrO_6 (Cr^{5+}) [2]	1.566	1.892	1.901	1.915	1.915	2.616
MoO_6 (Mo^{5+}) [3]	1.667	2.002	2.006	2.006	2.009	2.577

(a)

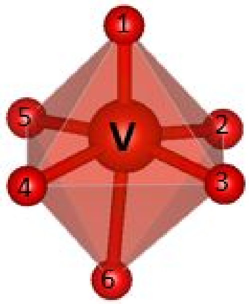

[1]

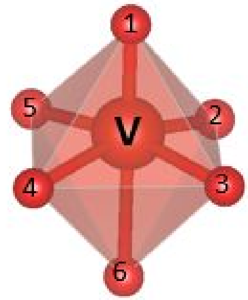

[2]

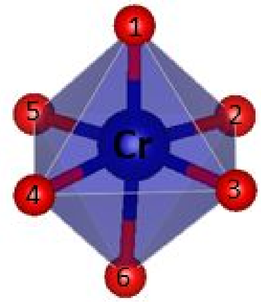

[3]

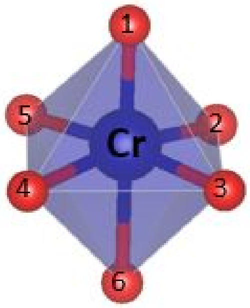

[4]

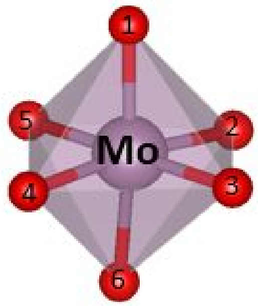

[5]

[6]

SYSTEM	Z-O_1 (Å)	Z-O_2 (Å)	Z-O_3 (Å)	Z-O_4 (Å)	Z-O_5 (Å)	Z-O_6 (Å)
V_1O_6 (V^{4+}) [1]	1.688	1.954	2.022	2.045	2.028	2.185
V_2O_6 (V^{4+}) [2]	1.686	1.990	2.008	2.063	1.992	2.179
Cr_1O_6 (Cr^{4+}) [3]	1.793	1.967	1.980	2.031	1.986	1.997
Cr_2O_6 (Cr^{4+}) [4]	1.779	1.993	1.989	2.060	1.980	2.032
Mo_1O_6 (Mo^{4+}) [5]	1.955	2.053	2.063	2.125	2.080	1.974
Mo_2O_6 (Mo^{4+}) [6]	1.950	2.093	2.060	2.155	2.043	2.000

(b)

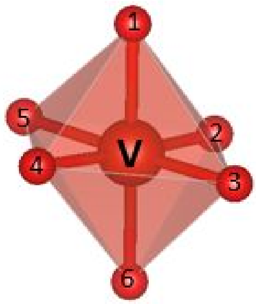

[1]

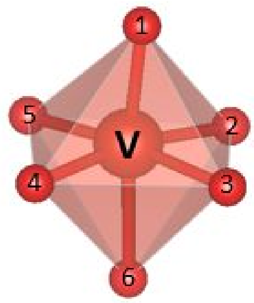

[2]

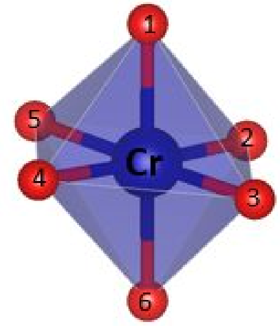

[3]

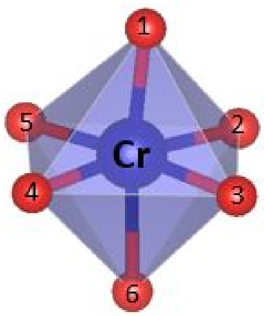

[4]

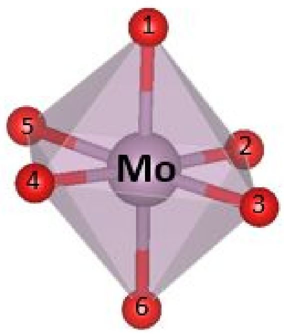

[5]

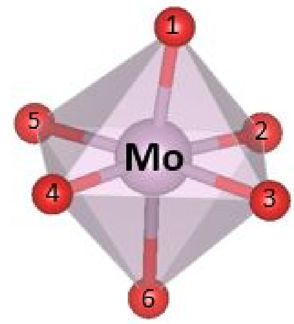

[6]

SYSTEM	Z-O_1 (Å)	Z-O_2 (Å)	Z-O_3 (Å)	Z-O_4 (Å)	Z-O_5 (Å)	Z-O_6 (Å)
V_1O_6 (V^{3+}) [1]	2.093	1.937	2.078	1.998	2.146	2.156
V_2O_6 (V^{3+}) [2]	2.034	1.998	2.135	1.945	2.088	2.229
Cr_1O_6 (Cr^{3+}) [3]	2.067	1.963	2.036	2.012	2.101	2.128
Cr_2O_6 (Cr^{3+}) [4]	2.043	2.008	2.074	1.970	2.052	2.168
Mo_1O_6 (Mo^{3+}) [5]	2.167	2.074	2.136	2.136	2.178	2.207
Mo_2O_6 (Mo^{3+}) [6]	2.135	2.117	2.163	2.083	2.151	2.212

(c)

Figure S2. (a) Local ZO_6 octahedral environments of $VOPO_4$ [1], Cr-$VOPO_4$ [2], and Mo-$VOPO_4$ [3]. This shows a clear Z=O oxo bond for all three cases. As a result, the O_6 atom is very far from the transition metal atoms; (b) Local ZO_6 octahedral environments of LiV_1OPO_4 [1], LiV_2OPO_4 [2], Cr_1-$LiVOPO_4$ [3], Cr_2-$LiVOPO_4$ [4], Mo_1-$LiVOPO_4$ [5], and Mo_2-$LiVOPO_4$ [6]. Again, we see the strong Z=O bonds to the O_1 atom, but now the O_6 atom is much closer for all cases; (c) Local ZO_6 octahedral environments of $Li_2V_1OPO_4$ [1], $Li_2V_2OPO_4$ [2], Cr_1-Li_2VOPO_4 [3], Cr_2-Li_2VOPO_4 [4], Mo_1-Li_2VOPO_4 [5], and Mo_2-Li_2VOPO_4 [6]. We no longer see the Z=O bonds but instead, a more perfect octahedral coordination for the t_{2g} occupied orbitals.

The unit cell data of ε-Li_xVOPO_4 is fairly consistent with the previously reported experimental and QM (HSE) derived cell parameters of Li_xVOPO_4 [1,4] .

The VO_6 environments at the 5+ oxidation state show one short V=O bond at 1.6 Å with four longer V-O bonds between 1.9 to 2.0 Å and one significantly longer bond at 2.6 Å. This is typical for a d^0 configuration in V.

For the 4+ oxidation state, we again find one short V=O bond at around 1.7 Å with four longer V-O bonds at 1.9 to 2.0 Å but now the O_6 atom is much closer with a distance at around 2.2 Å.

For the high spin 3+ oxidation state we find a rather symmetrical octahedral coordination of the V-O bonds with all six bonds ranging from 1.9 to 2.1 Å each.

The Cr-O bonds in CrO_6 for all oxidation states are generally similar in length to the V-O bonds showing that Cr is only slightly smaller than V.

The Mo-O bonds in MoO_6 are consistently longer than the V-O bonds by ~0.1 Å. The environments at the 5+ oxidation state highlight one short Mo=O bond at around 1.7 Å with four longer Mo-O bonds between 2.0 to 2.1 Å and the non-bonded O_6 atom that is 2.6 Å away.

For the Mo 4+ oxidation state, we find that the Mo-O bonds have a fairly symmetrical coordination with all six Mo-O bonds ranging from around 1.9 to 2.1 Å. This behavior is not found in either the V-O or Cr-O bonds at the 4+ oxidation state.

For the Mo 3+ oxidation state, we again see a symmetrical coordination of the O atoms with bonds ranging between 2.1 to 2.2 Å.

.

Electron Localization Function (ELF)

We assessed the electron localization using a topological display of the ELF [4,5] in which we sliced a 2-D plane through the transition metal atom and four of its oxygen neighbors at the dopant sites. Table S6 shows the exact Miller indices and vector distances from the origin "$\vec{d}$" to form the 2-D plane for each system. Because structural relaxation was slightly different for each system, the same Miller indices were not used to construct each 2-D plane but rather, the plane was fitted to the transition metal atoms and oxygen neighbors of interest specific to each system.

Table S6. Miller indices in the (hkl) plane format and vector distances from the origin for each constructed 2-D ELF plane

Lithium Content (x)	**System**	**h**	**k**	**l**	$\vec{d}$ **(Å)**
0	V	-1.183	5.360	-1	0.455
	Cr	1.237	-5.504	1	-0.455
	Mo	1.199	-5.618	1	-0.513
1	V_1	68.266	-1	-14.215	4.258
	V_2	-5.249	1	-2.081	-4.083
	Cr_1	141.112	-1	-24.690	4.318
	Cr_2	5.656	-1	2.306	4.157
	Mo_1	48.558	-1	-9.290	4.316
	Mo_2	5.675	-1	2.337	4.182
2	V_1	1	14.459	-1.078	4.602
	V_2	1	-5.289	-1.366	-6.488
	Cr_1	1.049	14.075	-1	4.619
	Cr_2	-1	5.157	1.328	6.476
	Mo_1	1.095	13.173	-1	4.643
	Mo_2	-1	4.744	1.229	6.551

References

(1) Lin, T.; Wen, B.; Wiaderek, K. M.; Sallis, S.; Liu, H.; Lapidus, S. H.; Borkiewicz, O. J.; Quackenbush, N. F.; Chernova, N. A.; Karki, K., et al. Thermodynamics, kinetics and structural evolution of ε-LiVOPO4 over multiple lithium intercalation. *Chem. Mater.* **2016,** *28*, 1794-1805.

(2) Urban, A.; Seo, D.; Ceder, G. Computational understanding of li-ion batteries. *Npj Comput. Mater.* **2016**, *2*, 16002.

(3) Aydinol, M. K.; Kohan, A. F.; Ceder, G.; Cho, K.; Joannopoulos, J. Ab initio study of lithium intercalation in metal oxides and metal dichalcogenides. *Phys. Rev. B Condens. Matter* **1997**, *56*, 1354--1365

(4) Bianchini, M.; Ateba-Mba, J. M.; Dagault, P.; Bogdan, E.; Carlier, D.; Suard, E.; Masquelier, C.; Croguennec, L. Multiple phases in the ϵ-VPO4O - LiVPO4O - Li2VPO4O system: a combined solid state electrochemistry and diffraction structural study. *J. Mater. Chem. A* **2014**, *2*, 10182.

(5) Ling, C.; Zhang, R.; Mizuno, F. Phase stability and its impact on the electrochemical performance of $VOPO_4$ and $LiVOPO_4$†. *J. Mater. Chem. A* **2014,** *2*, 12330.

(6) Harrison, K. L.; Bridges, C. A.; Segre, C. U.; Varnado, C. V.; Applestone, D.; Bielawski, C. W.; Paranthaman, M. P.; Manthiram, A. Chemical and electrochemical lithiation of LiVOPO4 cathodes for lithium-ion batteries. *Chem. Mater.* **2014,** *26*, 3849-3861.

(7) Sargsyan, K.; Grauffel, C.; Lim, C. How molecular size impacts RMSD applications in molecular dynamics simulations. *J. Chem. Theory Comput.* **2017,** *13,* 1518-1524.